TRIMICROSTRIP TRI-BAND COUPLERS ON COPLANAR WAVEGUIDE AND SLOTLINE TECHNOLOGIES FOR 3 dB, 6 dB, AND 10 dB APPLICATIONS

Rahmouna EL BOUSLEMTI [1, *], Mehdi Chemseddine FARAH [2]

In this paper, the configuration of microstrip/slotline transitions is used to describe and design our couplers through two proposed transmission line models, a directional microstrip coupler named A and a coupler with microstrip slotline named B, which have a simple structure operating in the 3-11 GHz frequency band. The design parameters were calculated using Ansoft HFSS. Experimental results on the proposed 1 dB and 3 dB directional couplers designed from these calculations demonstrated fairly satisfactory agreement with predictions. The slot line leads to better coupling and good isolation at 3.6 GHz, justifying that the slotline transition configuration offers better coupler performance.

Keywords: 3-dB Directional Coupler, Microstrip, Slotline, S-Parameters

1. Introduction

The slotline was first developed in the field of microwave circuit design. It appeared in technical literature in the 1950s, as mentioned in [1]. Several researchers have begun to explore this technique to design microwave components, such as filters and power dividers. Their work was grouped and published by the American Department of Defense in 1971, as presented in [2].

The slotline is used in a variety of applications, including the design of microwave filters, power dividers, directional couplers, and other microwave circuit components [3-6]. It is often used when specific coupling or filtering characteristics are required.

Over the years, the design and analysis of slotlines have evolved with the advancement of microwave technology and high-frequency electronics, as presented in [7–10]. Engineers continue to develop new techniques for designing and optimizing slotlines to meet the growing needs of wireless communication, radar technology, remote sensing, and other related fields.

[1, *] Prof., Telecommunications and Digital Signal Processing Laboratory, Djillali Liabes University, Sidi Bel Abbes, Algeria, and Department of process and materials engineering, National Polytechnic School of Oran, Algeria, e-mail: rahmouna.elbouslemti@enp-oran.dz

[2] Prof., Telecommunications and Digital Signal Processing Laboratory, and Department of Telecommunications, Djillali Liabes University, Sidi Bel Abbes, Algeria, e-mail: mehdi.farah@univ-sba.dz

The slotline is one of many elements of microwave technology that has a rich history and continues to be an essential part of microwave component design, such as the directional coupler, which will be presented and studied in this work.

The directional coupler is designed to split an incoming RF signal into two or more outputs with minimal insertion loss. It usually has a main output where most of the signal is transmitted, a measurement output where a small portion of the signal is directed to be measured, and sometimes one or more isolated outputs where the signal is reflected and dissipated.

Directional couplers are widely used in RF and microwave applications, including telecommunications systems, wireless networks, radar, RF measurement instruments, and more. They allow the power of the transmitted signal to be accurately measured without interrupting the main signal flow. There are different types of directional couplers, such as slot-directional couplers, resonator-directional couplers, stripline-directional couplers, and others. Each type has specific characteristics in terms of bandwidth, insertion loss, and isolation between transmission lines.

In this paper, the planar directional couplers width coupling slots were specifically designed to have tri-band operation where the classical structure of the coupler has been modified and improved. The coupling slot is the slot that is located on the upper wall of the structure, as mentioned by the separation between the two conductive lines, which contains ports 1 and 2 on the one hand and, on the other hand, contains ports 2 and 4. This spacing is mentioned in this work by slot. The particular coupler width coupling slots are discussed in [11]. They are built on a folded half-mode substrate integrated waveguide (FHMSIW) structure.

In recent research work, a few designs of power dividers and couplers using slotline transition have been proposed [12, 13, 14] and realized on different substrates. In [15], the authors realized a balanced-to-balanced filtering directional coupler based on microstrip/slotline transition structures, resonance structures, and odd-even mode phase velocity compensation structures.

Very few research papers have studied directional couplers based on slotline transitions, as cited in [16, 17]. In the following section, the operating principle and its theoretical background are presented. In the third part, a parametric analysis of this device is carried out. Finally, we conclude with our results and indicate future perspectives and improvements.

2. Objective

The objective of our work is to

- Create a design of two miniature directional couplers of different types, one without a slot in the ground and the other with a slot using slotline transition, and do the numerical modeling in planar technologies while improving their performances.

- Production of the proposed components.
- Have a tri-band operation.

3. Key Contributions and Performance Comparison

In this study, we introduce microstrip/slotline directional couplers designed to operate in three distinct frequency bands: 3.6 GHz, 6.8 GHz, and 9 GHz. This tri-band capability sets our work apart, as it provides enhanced versatility for a variety of RF applications. While most previous research has focused on couplers with a narrower frequency range, typically operating in just one or two bands, our approach offers a significant improvement by incorporating multi-band functionality. This is a key advantage for modern communication systems that rely on devices capable of handling multiple frequency bands simultaneously.

In addition, we were able to compare our work with that presented in [18] and [19]. There is very little research on slotline couplers; most work has studied slotline power dividers. The table below provides the comparison results.

Table 1

Comparative evaluation of various couplers

Reference	[18]	[19]	This work
Operating frequencies (GHz)	1.2/ 2.52	1.65/3.30	3.6/ 6.8/ 9
Isolation (dB)	-25	-42.41	-31.82
Insertion loss (dB)	-1.5	--2.29	-1.20
Coupling loss (dB)	-5.30	-3.75	-3.64
Perfect impedance matching	Yes	Yes	Yes
slotline transmission	No	No	Yes

Table 1 presents a comparative evaluation of the performances of the couplers proposed in the works of [18, 19], and this study. When comparing the coupler performances, it is clear that although the operating frequencies differ between the studies (1.2/2.52 GHz and 1.65/3.30 GHz in [18] and [19], respectively, versus 3.6/6.8/9 GHz in this study), all configurations achieve perfect impedance matching, suggesting that each design has been optimized for optimal operation within its respective frequency range. Regarding isolation, our work achieves -31.82 dB, which is better than [18] (-25 dB), but slightly lower than [19] (-42.41 dB). This difference can be explained by the use of slotline transmission in our design, which allows for competitive performance while reducing insertion losses. On the other hand, the insertion losses in our work are -1.20 dB, which is better than [18] (-1.5 dB), but still lower than [19] (-2.29 dB). This result indicates that the addition of slots for transmission improves losses compared to other designs, although there is still room for improvement. Finally, the coupling losses

in this work are -3.64 dB, a competitive result compared to the other works, where the coupling losses are -5.30 dB in [18] and -3.75 dB in [19]. The design proposed in this study thus offers an optimal combination of performance, particularly in terms of isolation, insertion losses, and coupling losses, while introducing slotline transmission, an innovation that allows for more efficient coupling management. The results obtained demonstrate that this approach represents a significant improvement over previous designs, especially in terms of impedance matching and insertion losses.

4. Theory and design

A directional coupler operates by distributing the power of the RF signal at the input of channel 1 in a controlled manner between two channels, main and secondary. This operation ensures that there is no power delivered to the fourth port where there is isolation ; there is no power that can be delivered to Port 2 (isolation).

Several variables can be used to define the transmission line characteristics of a directional coupler and evaluate its performance.

The characteristic impedance of a microstirp structure, studied by Bahl and Trivedi in [20], is given by :

For $W/h \geq 1$,

$$Z_0 = \frac{120\,\pi/\sqrt{\varepsilon_{eff}}}{W/h+1.393+0.667\,\ln(W/h+1.444)} \quad (1)$$

Where W is the width of conducting line, mentioned by ω in Fig. 3, and h is the height of dielectric substrate.

ε_{eff} is the effective relative permittivity and ε_r is the relative dieclectric constant

$$\varepsilon_{eff} = \frac{\varepsilon_r+1}{2} + \frac{\varepsilon_r-1}{2}\left(1+12\,\frac{h}{w}\right)^{-1/2} \quad (2)$$

We use (1) et (2) to calculate the characteristic impedance of our directional coupler, given in Fig 2. The Z_c must be equal to 50 for w= 3 mm.

The characteristic impedance of the proposed coupler and that of the coupler with slotline are equal, given by:

$$Z_0 = Z_S = 50\Omega \quad (3)$$

It is convenient to introduce normalized impedance factors for the slotline stub, which is shown in Fig. 3, and the closed microstrip stub, respectively [21].

$$\wp = \frac{Z_S}{50\Omega} \quad (4)$$

$$\omega = \frac{50\Omega}{Z_0} \quad (5)$$

It has to be noted that the length of the stub of the conductive line is equal to that of the stub of the slotline, which is on the lower face.

We can give the value of the transmission coefficient as given in [21]:

$$|S_{21}| = \frac{1}{\sqrt{1+\frac{1}{\wp^2}\frac{cot^2\beta.L}{4}}} \quad (6)$$

We have : $\wp = cot\ \beta.L$ (7)

with β is the bandwidth.

Leading to a value of β :

$$\beta = \frac{f_2|_{dB}}{f_1|_{dB}} \quad (8)$$

f_1 and f_2 are the bandwidth limits of the insertion loss, correspond to 1.20 dB around 3.6 GHz.

The cutoff frequency is calculated using the equation cited in [22]:

$$f_c = \frac{C}{4L_c\sqrt{\varepsilon_r}} \quad (9)$$

C is the speed of light, and L_c is the length of the coupling line.

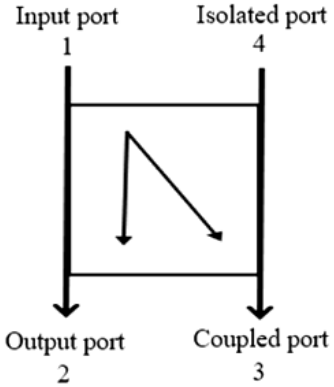

Fig. 1. Directional coupler

5. Design of a microstrip coupler

To obtain a good directional coupler, it is important to satisfy several essential conditions, including low insertion losses, adequate coupling between the main channel and the auxiliary channel, low return loss, and good impedance matching. By meeting these conditions, a directional coupler can operate efficiently and precisely.

Here, we will take a closer look at the proposed A and B directional coupler designs, highlighting the features that set them apart and the benefits they offer to

meet the specific needs of our study. These proposed couplers comply with the operating conditions cited above. The proposed couplers operate at three frequencies: 3.6 GHz, 6.8 GHz, and 9 GHz. These particular frequency values were chosen because they are critical for modern communication systems, including 5G networks, radar systems, and satellite communications.

The tri-band functionality of the couplers offers significant advantages by enabling multi-band operation. This allows the couplers to support diverse applications without the need for multiple distinct devices. The ability to efficiently operate across these three frequencies enhances the flexibility of the system, ensuring its relevance to current and future RF technologies.

Figs. 2 and 3 illustrate the microstrip configuration selected for manufacturing the directional coupler prototypes. Fig. 2 shows the configuration of the proposed coupler A. It includes two views: (A) the top view and (B) the 3D view. The top view (A) represents the geometry of coupler A, showing the main and auxiliary transmission lines, along with the central conductors that divide the input signal between ports 2 and 3. The 3D view (B) provides a complete spatial representation of the coupler, showing the transmission lines, connections, and specific component dimensions.

Fig. 3 shows the configuration of the proposed coupler B. It represents the top view of the geometry, with a slot above the access lines. This slot is characterized by its width (w1) and its length (Ls), which are crucial parameters in the design. These dimensions help optimize coupling efficiency and reduce insertion losses. Additionally, the slot is positioned on the lower ground plane, and its role is to facilitate effective coupling between the main and auxiliary channels of the coupler.Remember that the directional coupler without a slot in the lower mass is named coupler A, and the coupler with a coupling slot is named coupler B.

These two couplers are designed to operate at 3.6, 6.8, and 9 GHz.

Table 2 shows the geometric parameters of the proposed couplers that were found by using Ansoft HFSS (High Frequency Electromagnetic Field Simulation) to do 3D electromagnetic simulations and find the best ones.

The devices are composed of a direct transmission line from port 1 to port 2, a coupling line from port 1 to port 3, and a central conductor with a casi-circular shape located at the level center of the top surface.

The input signal from port 1 is split between ports 2 and 3 via the transition and coupled lines. The characteristic impedances are equal to 50 according to the theoretical formulas (1) and (2).

The line of slots necessary for transitions at the lower layer ends with open circuits made using two radial slots.

The B coupler design is based on a combination of microstrip transmission lines with slotted lines, which ensures an efficient line-to-slot transition while providing low insertion loss.

An innovative design is shown in Fig. 2. The ground plane's microstrip serves as the slot's termination, terminating in an open circuit. The slot, which ends in an open circuit, extends through the ground plane of the microstrip above the center lines.

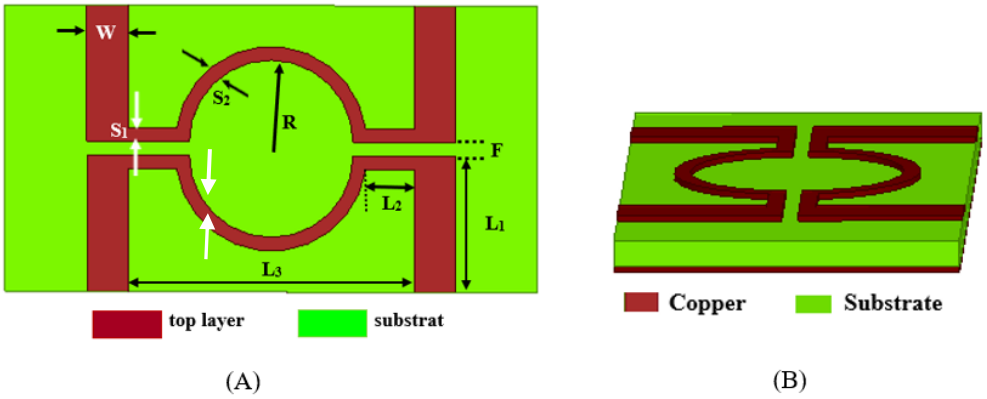

Fig. 2. Configuration of the proposed coupler A, (A) Top and (B) 3D view

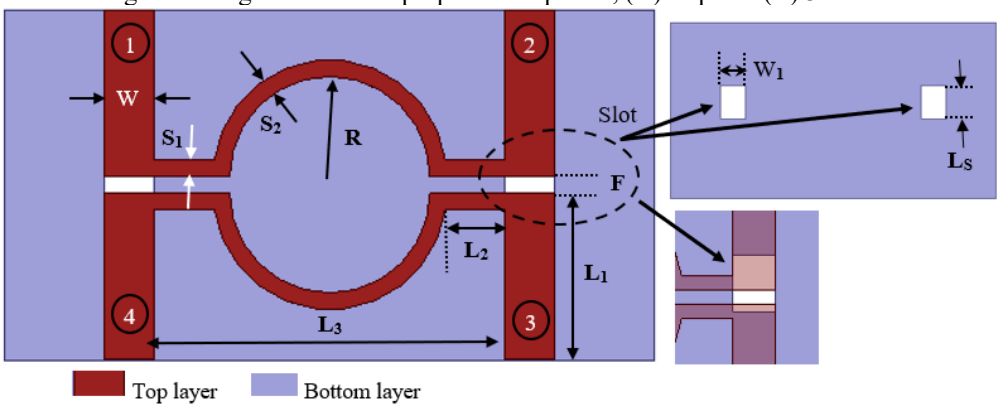

Fig. 3. Configuration of the proposed coupler B

The characteristic impedance of the slotline is calculated with the equation in [22].

$$\omega = \wp\left(1 + \frac{cot^2\beta.L}{\wp^2}\right) \tag{10}$$

We can deduce an optimal relationship between the two impedance factors by substituting equation (7) into equation (10), which leads to:

$$\omega = 2.\wp \tag{11}$$

An optimum value of S21 is [22]:

$$|S_{21}| = \frac{1}{\sqrt{1+\frac{1}{4\wp^2}\frac{cot^4\beta.L}{\wp^2+cot^2\beta.L}}} \quad (12)$$

6. Manufacturing and Measurements

In order to validate our design, couplers A and B in microstrip PCB technology operating in Tri-Band are manufactured on an FR4 substrate with a relative permittivity of, a loss tangent of 0.025, and a thickness of 1.5 mm.

The final physical dimensions of the two proposed models are listed in Table 2.

Table 2

Design parameters are expressed in milimeters

Parameters	Coupler		
	A	B	
W	3	3	
L_1	10	10	
L_2	3.75	2	
L_3	21	19	
S_1	1	1	
S_2	1	1	
F	1	1	
R	6	6	
Slot		W_1 3	Ls 4

Based on the physical parameters shown in Table 2 and the theory given above, both couplers are analytically modeled using HFSS, fabricated, and experimentally tested to operate in the 0 – 11 GHz band. Coupler B is designed using a slotline, as shown in Fig. 3.

In this design process, mutual transmission between the signal-carrying line and the coupled line must be ensured, and isolation optimization is necessary.

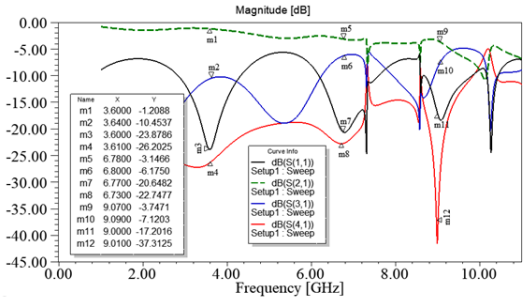

Fig. 4. Simulated results of the coupler A

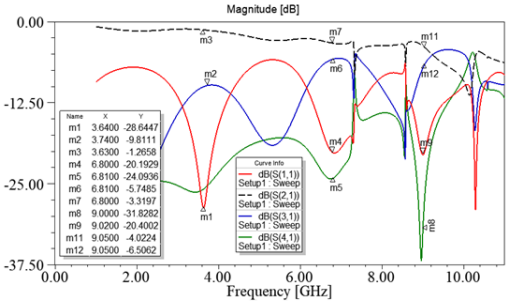

Fig. 5. Simulated results of the coupler B

The experimental structures consist of an excitation line soldered to the SMA connector. The transmission parameters S are measured with a network analyzer (E5071C).

Figs. 4 and 5 show the simulated performances of Coupler A and Coupler B, respectively. Photos of the proposed experimental prototypes with their top and bottom views are given in Figs. 6 and 7. The size of fabricated couplers is 20×26.3 mm^2.

The comparison between the simulated and measured performances of Coupler A and Coupler B is shown in Figs. 8 and 9, respectively. These figures present the evolution of the S-parameters across the operating frequency band. Overall, the results demonstrate a good agreement between simulations and measurements, confirming the reliability of the proposed designs. Figs 8(a) and 9(a) illustrate the coupling coefficient S31, which corresponds to the transmission between the input port (Port 1) and the coupled port (Port 3).

Figs. 8(b) and 9(b) show the insertion loss S21, representing the transmission from the input port (Port 1) to the through port (Port 2). Across a bandwidth of approximately 6.8 GHz, the insertion loss varies between -0.8 dB and -4.5 dB, which indicates acceptable transmission performance for both couplers. The isolation performance, represented by S41, is shown in Figs 8(c) and 9(c). In both cases, the isolation exceeds 20 dB across the working frequency band, which reflects the good isolation capability of the devices. Finally, Figs 8(d) and 9(d) display the return loss S11, indicating the impedance matching at the input port. The results confirm good matching over the entire operational frequency range. The exact simulated and measured values of S21, S31, S41, and S11 at the operating frequencies are already provided in Tables 3, 4, and 5. This agreement between simulation and measurement confirms the effectiveness of the proposed couplers.

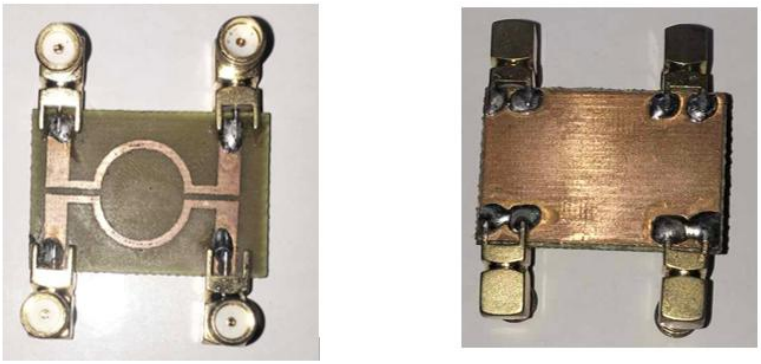

Fig. 6. Photograph of the fabricated coupler A: (left) top face; (right) bottom face

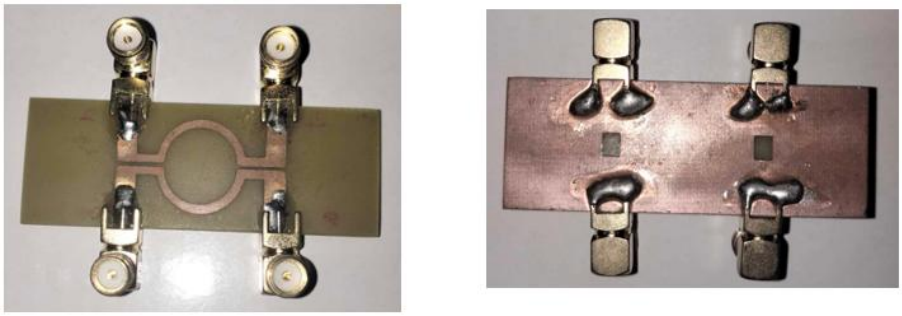

Fig. 7. Photograph of the fabricated coupler B: (left) top face; (right) bottom face

The size of coupler A is 20×25 mm^2, while the size of coupler B without the four ports and the added space that exceeds the ports is estimated to be 14 mm. In fact, its size has been significantly reduced. According to the results obtained and illustrated in tables 3, 4, and 5, it is observed that there is a reasonable agreement between simulation and experiment.

We observe that there are ripples in the frequency response of the two couplers. It is notable for Response S21. Soldering the SMA connectors is a potential cause of this. This effect affects all the S parameters of the transition, especially S41 and S21.

Table 3

Performance of the proposed couplers at 3.6 GHz

Sim			Meas		
S IJ [dB]	Coupler A	Coupler B	**S** IJ [dB]	Coupler A	Coupler B
S21	-1.20	-1.26	S21	-1.58	-1.83
S31	-3.64	-9.01	S31	-1.13	-10.10
S41	-26.20	-25.88	S41	-20.96	-19.24
S11	-23.87	-28.64	S11	-16.97	-19.81

Table 4

Performance of the proposed couplers at 6.80 GHz

Sim			Meas		
S IJ [dB]	Coupler A	Coupler B	**S** IJ [dB]	Coupler A	Coupler B
S21	-3.14	-3.31	S21	-5.08	-4.58
S31	-6.17	-5.74	S31	-7.50	-7.80
S41	-22.74	-24.08	S41	-27.20	-17.75
S11	-20.64	-20.19	S11	-22.13	-20.98

Table 5

Performance of the proposed couplers at 09 GHz

Sim			Meas		
S IJ [dB]	Coupler A	Coupler B	**S** IJ [dB]	Coupler A	Coupler B
S21	-3.74	-4.01	S21	-6.09	-7.35
S31	-6.80	-6.50	S31	-1.08	-1.08
S41	-37.31	-31.82	S41	-28.90	-21.85
S11	-17.20	-20.40	S11	-17.60	-15.90

For the operating band from 3 GHz to 9.5 GHz, the values of the simulated and measured S21 insertion losses of the two couplers A and B are better, which reach 1.2 dB and 3 dB for the frequencies 3.6 and 6.8 GHz, respectively, and 4 dB at 9 GHz. The S31 transmission losses on the coupled line are 3.6 dB at 3.6 GHz and 6.8 dB at 3.6 and 9 GHz. These values represent the good transmission performance of the proposed couplers. The simulated and measured isolations between S41 input 1 and output 4 ports are both greater than 20 dB at all three operating frequencies. Additionally, the simulated and measured reflection losses are greater than 20 dB. Furthermore, the measured phase difference for the two couplers A and B is shown in Fig. 10, which shows that the phase difference is approximately 91° at 3.6 GHz, 87.89° at 6.8 GHz, and 100° at 9 GHz. A good phase difference response is observed at the 3.6 GHz frequency for the couplers proposed.

According to the comparison between the results found for the two couplers A and B, we notice that the two couplers have good performances at the three operating frequencies, but the best values are observed at 3.6 GHz.

The measured isolation is very acceptable, which seems to demonstrate the effectiveness of slotted lines.

All the S parameters of the B coupler prove good efficiency and better performance, which seems to prove that the coupler, whether with or without slot, has the capacity to ensure a transition of 1, 3, and 9 dB and to operate at 3 different frequ encies.

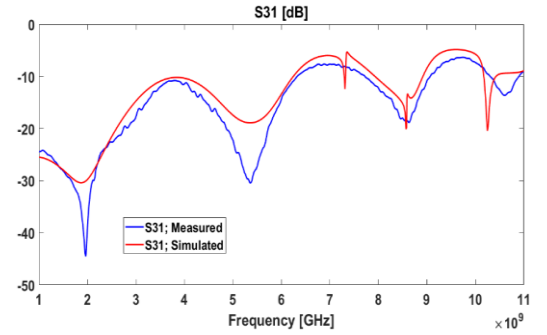

(a)

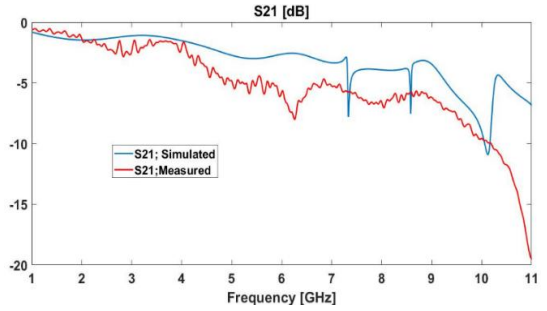

(b)

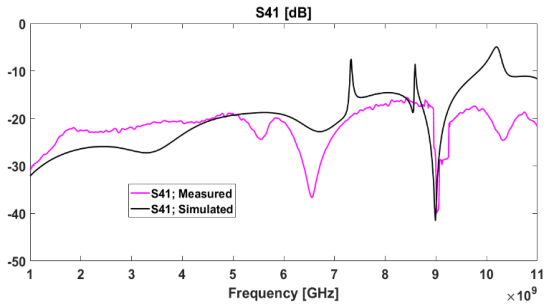

(c)

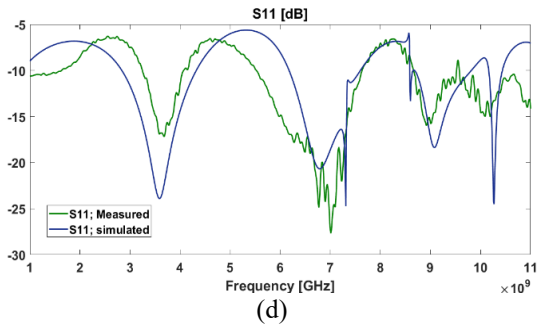

(d)

Fig. 8. Performances of Coupler A at 3.6 GHz, 6.8 GHz, and 9 GHz, respectively: Magnitude of (a) S31; (b) S21, (c) S41, and (d) *S*11.

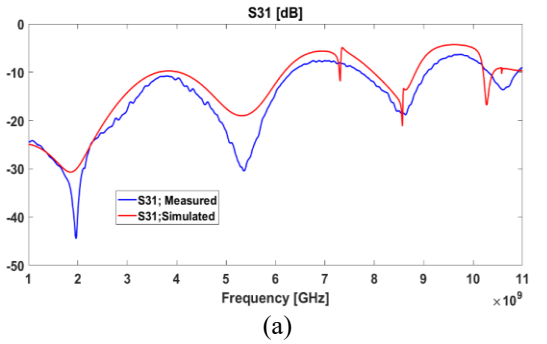

(a)

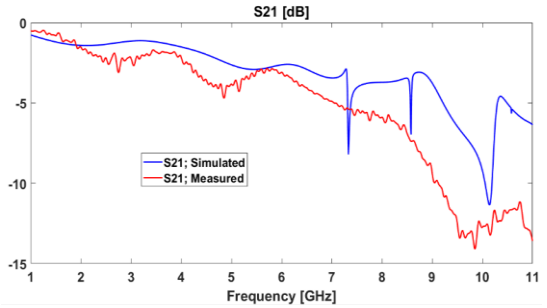

(b)

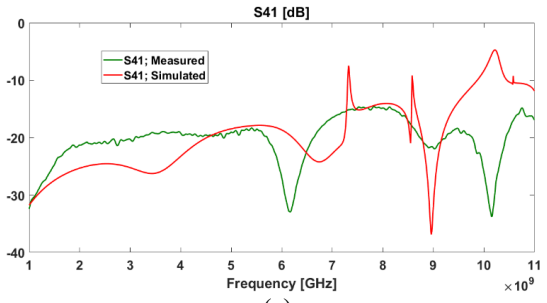

(c)

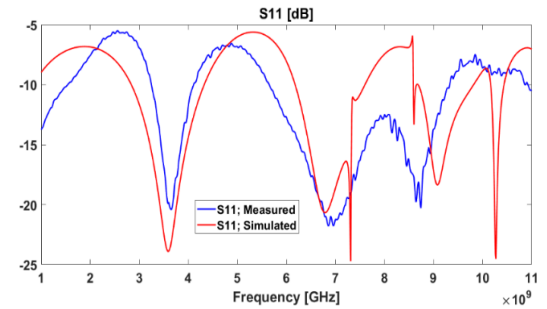

(d)

Fig. 9. Performances of Coupler B at 3.6 GHz, 6.8 GHz, and 9 GHz, respectively: Magnitude of (a) S31; (b) S21, (c) S41, and (d) *S*11.

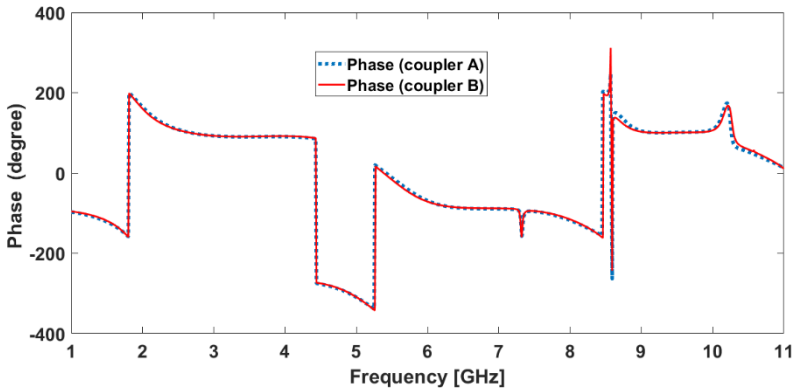

Fig. 10. Phase differences

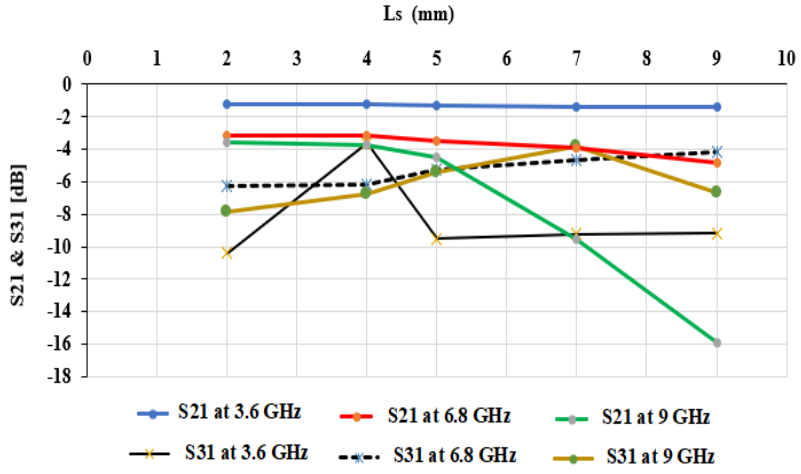

Fig. 11. Impact of the variation in the width of the Ls on S21 and S31

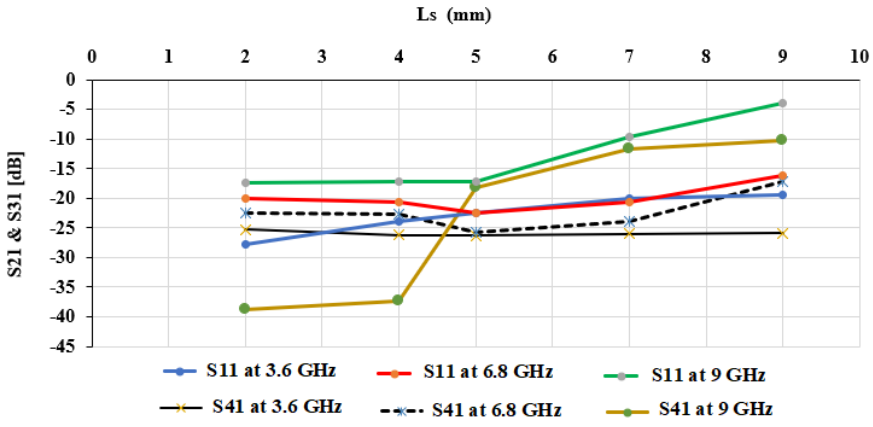

Fig. 12. Impact of the variation in the width of the Ls on S11 and S41

To validate our design as effectively as possible, we pay particular attention to three essential elements: functionality, manufacturability, and feasibility of the proposed couplers.

The results cited in this article validate the design, manufacturing, and proper functioning of the components. To validate their feasibility, we must study the variation of the length of the slot Ls in order to evaluate its influence on the performance of the coupler B with slotline.

Figs.. 11 and 12 illustrate the effect of varying the width of the Ls on the operating frequencies at 3.6, 6.8, and 9 GHz. Changes in the length of this segment influence the S parameters of the considered slotline coupler.

We observe that by increasing the length of the segment, the reflection loss and the isolation gradually decrease, but the coupler does not give good results, which ensures poor power transmission at the 9 GHz frequency. On the other hand, there is an improvement in the S parameters for the 6.8 GHz frequency. Consequentially, to operate at three different frequencies, it is necessary to choose the value of the segment Ls that does not exceed the value of the signal line.

6. Conclusions

In this paper, two microstrip directional couplers are proposed and implemented. using a typical printed circuit board manufacturing process, PCB technology successfully manufactures the proposed couplers.

A slotline transmission line is designed to design the second coupler. The results report that the designed transmission lines exhibit satisfactory transmission characteristics and a 90-degree phase shift at particular operating frequencies.

The simulated and measured results are encouraging and show good agreement. Which validates our study. As a result, the proposed couplers have good reflection and insertion loss performance and satisfactory isolation. This can more accurately evaluate the efficiency of the slotline, which exhibits satisfactory transmission performance for coupler B.

Acknowledgment

This work was supported by Directorate General for Scientific Research and Technological development (DGRSDT)(Algeria).

R E F E R E N C E S

[1] *E. Strumwasser, J. A. Short, R. J. Stegen, and J. R. Miller*, Slot study in rectangular TEM transmission line, Hughes Aircraft Company, Tech. Memo 265, Air Force Contract AF, Vol. **19**, Iss. 122, 1952, DOI: 10.21236/ADA800343.

[2] *E. G. Cristal, D. K. Adams, R. Y. C Ho and S. B. Cohn*, Microwave synthesis techniques annual report; united states army electronics command fort monmouth, N.J. 07703, 1968.

[3] *E. G. Cristal, D. K. Adams*, *R. Y. C Ho and S. B. Cohn*, Microwave synthesis techniques, stanford research institute, September 1968.
[4] *B. Seymour. Cohn*, Slot Line on a Dielectric Substrate, IEEE transactions on microwave theory and techniques, Vol. **mtt-17**, Iss. 10, 1969, DOI: 10.1109/TMTT.1969.1127058.
[5] *B. Jeffrey Knorr*, Slot-Line Transitions, IEEE transactions on microwave theory and techniques, Vol. **22**, Iss. 5, 1974, DOI: 10.1109/TMTT.1974.1128278.
[6] *M. M. Zinieris, R. Sloan, and L. E. Davis*, A broadband microstripto-slot-line transition**,** microwave and optical technology letters, Vol. **18**, Iss. 5, 1998.
[7] *R. M. Garg, I. Bahl et M. E. Bozzi*, Microstrip Lines and Slotlines, Artech House, 2013.
[8] *B. Schiek and J. Kodhler*, An Improved Microstrip-to-Microslot Transition, IEEE transactions on microwavs thsory and techniques, Vol. **24**, Iss. 4, 1976, DOI: 10.1109/TMTT.1976.1128823.
[9] *P.H Wen, C.I. G. Hsu, C.H. Lee, and H.H. Chen,* Design of balanced and balun diplexers using stepped-impedance slot-line resonators, Journal of Electromagnetic Waves and Applications, Vol. **28**, Iss. 6, 2014, DOI: 100140. 10.1080/09205071.2014.885398.
[10] *K. Song, and Q. Xue*, Novel Ultra-Wideband (UWB) Multilayer Slotline Power Divider With Bandpass Response, IEEE microwave and wireless components letters, Vol. **20**, Iss. 1, 2010, DOI: 10.1109/LMWC.2009.203595.
[11] *W. Hong, Min Hua Ho, and J. J. Feng*, wideband coupler of folded half mode substrate integrated waveguide design with combined microstrip and stripline feed, Microwave and optical technology letters, Vol. **58**, No. 5, 2016.
[12] *L. Xiao, H. Peng, T. Yang, and J. Dong*, Power Divider Based on Stepped-Impedance Slotline, Progress in Electromagnetics Research C, Vol. **50**, 2014.
[13] *L. Guo, A. Abbosh and H. Zhu*, Ultra-wideband in-phase power divider using stepped-impedance three-line coupled structure and microstrip-to-slotline transitions, Electronics letters 27th ,Vol. **50**, Iss. 5, 2014, DOI : 10.1049/el.2013.4160
[14] *F. Lin, Q. X. Chu, Z. Gong, and Z. Lin*, Compact broadband Gysel power divider with arbitrary powerdividing ratio using microstrip/slotline phase inverter, IEEE Trans. Microw. Theory Tech, Vol. **60**, 2012, DOI: 10.1109/TMTT.2012.2187067.
[15] *L. Qiao, R. Li, Y. Han, F. Wei, Y. Yang, X. Yang and N. Wu*, A Balanced Filtering Directional Coupler withWide Common-Mode Suppression Based on Slotline Structure, Electronics, Vol. **10**, 2254, 2021, Doi :10.3390/electronics10182254.
[16] *G.Q. Liu, L.S. Wu and* W.Y. Yin, A compact microstrip rat-race coupler with modified lange and t-shaped arms, Progress In Electromagnetics Research, Vol. **115**, 2011, Doi:10.2528/PIER11032003.
[17] *F. Lin, Q.-X. Chu and S.W. Wong*, Compact broadband microstrip rat-race couplers using microstrip/slotline phase inverters for arbitrary power-dividing ratios, Journal of Electromagnetic Waves and Applications Vol. **26**, 17–18, 2358–2364, 2012.
[18] *J. Zhang, T. Jianfeng, B. Zong, and C. Zhou*, Compact Branch-Line Coupler Using Uniplanar Spiral Based CRLH-TL, Progress In Electromagnetics Research Letters, Vol. **52**, 2015, DOI:10.2528/PIERL15011414.
[19] *R. El Bouslemti and F. Salah-Belkhodja*, Design, simulation and realization of a compact dual band meandered coupler, J. Fundam. Appl. Sci., Vol. **11**, Iss. 3, 2019, Doi : 10.4314/jfas.v11i3.16
[20] *I. J. Bahl and D.K. Trivedi*, A designers's Guides to Microstrip line, Microwave, Vol. **16**, Iss. 5, 1977.
[21] *K.C. Gupta, R. Garg, I. Bahl and P. Bhartia*, Microstrip Lines and Slotlines, 2nd ed, Artech House. INC, 269-340, 1996.

[22] *B. Schuppert*, Micros trip / Slotline Transitions: Modeling and Experimental Investigation, IEEE transactions on microwave theory and techniques, Vol. 36, Iss 8, 1988, DOI: 10.1109/22.3669.
[23] *I. A. Mocanu,* The influence of cell symmetry in the performances of d-crlh branch line couplers, U.P.B. Sci. Bull., Series C, Vol. **74**, Iss. 2, 2012.
[24] *B. Nataraj, K. Porkumaran*, Investigation of using tapered coplanar waveguide in rf mems phase shifter, U.P.B. Sci. Bull., Series C, Vol. **75**, Iss. 1, 2013.